dentistry journal

MDPI

Article

Effects of 3D-Printing Orientation and Materials Selection on Microbial Accumulation of Customized Healing Abutments: An In Vitro Comparative Study

Faisal E. Aljofi

Department of Preventive Dental Sciences, College of Dentistry, Imam Abdulrahman Bin Faisal University, P.O. Box 1982, Dammam 31441, Saudi Arabia; fealjofi@iau.edu.sa

Abstract

Objectives: To evaluate the effect of different healing abutment materials and 3D-printing orientations on microbial accumulation by comparing commercially available titanium abutments with customized composite resin and 3D-printed healing abutments. **Methods:** Fifty healing abutments were allocated into five groups ($n = 10$): commercially available titanium (control), customized healing abutment resin composite CHA-Composite, and 3D-printed customized healing abutments printed in 0°, 45°, and 90° orientations (CHA-3DP-0, CHA-3DP-45, CHA-3DP-90). Following sterilization, specimens were incubated with standardized suspensions of *S. aureus* and *C. albicans* for 24 h. Adherent microorganisms were quantified by colony-forming unit (CFU) analysis, and representative specimens were examined using scanning electron microscopy (SEM). Data were analyzed using one-way ANOVA with Tukey's post hoc test ($\alpha = 0.05$). **Results:** Significant differences in microbial accumulation were observed among the experimental groups for both *C. albicans* and *S. aureus* ($p < 0.001$). The 3D-printed healing abutments at the 0° orientation demonstrated the lowest CFU counts for both microorganisms, significantly lower than all other groups ($p < 0.001$). In contrast, the 45° and particularly the 90° printing orientations exhibited significantly greater microbial accumulation. SEM findings corroborated the quantitative results, revealing reduced biofilm accumulation on 0°-3D-printed surfaces and more extensive biofilm formation on the 45° and 90° groups. **Conclusions:** Healing abutment material and manufacturing method, as well as 3D-printing orientation, were associated with differences in early microbial accumulation. Among the 3D-printed groups fabricated from the same resin, the 0° printing orientation showed the lowest *S. aureus* and *C. albicans* accumulation, suggesting that optimized printing orientation may reduce microbial accumulation. As the titanium, composite resin, and 3D-printed groups differed simultaneously in both material and fabrication method, these comparisons should be interpreted as reflecting specific material–manufacturing process combinations rather than an independent material effect. Further clinical and in vitro investigations are needed to confirm these findings.

Keywords: additive manufacturing; colony-forming unit; peri-implantits; peri-implant mucositis; dental composite healing abutment; microbial; stock healing abutment

Check for updates

Academic Editors: Hans S. Malmstrom and Andrea Scribante

Received: 1 August 2026
Revised: 13 November 2026
Accepted: 18 November 2026
Published: 23 November 2026

Copyright: © 2026 by the author. Licensee MDPI, Basel, Switzerland. This article is an open access article distributed under the terms and conditions of the Creative Commons Attribution (CC BY) license.

1. Introduction

Dental implants are widely recognized as a predictable and effective treatment for replacing missing teeth, restoring both masticatory function and esthetics. However, the

long-term success of implant therapy extends beyond osseointegration and relies on the preservation and stability of the surrounding peri-implant hard and soft tissues [1]. During the healing period between implant placement and definitive prosthetic restoration, various surgical and prosthetic strategies have been introduced to support soft tissue maturation, preserve peri-implant architecture, and facilitate the development of an optimal emergence profile [2–5].

After placement of endosseous dental implants, healing abutments are routinely connected during the transmucosal healing phase and maintained until fabrication of the definitive prosthesis. Their primary function is to promote the maturation and maintenance of the peri-implant soft tissue architecture while preserving the stability of the surrounding hard tissues [6,7]. For that, a variety of materials and techniques have been introduced and used [3,4,8,9]. These strategies encompass both prefabricated commercially available healing abutments manufactured from titanium or titanium alloys due to their excellent biocompatibility, corrosion resistance, and mechanical properties and customized healing abutments (CHAs) fabricated from materials such as resin composites, auto-polymerized poly (methyl methacrylate) (PMMA) resin, Polyetheretherketone (PEEK), Zirconia and three-dimensional (3D)-printed biomaterials using CAD-CAM technology, allowing individualized soft tissue contouring and emergence profile development [2,5,9,10].

The diverse materials used during the peri-implant healing phase are continuously exposed to the oral environment, rendering them susceptible to colonization by a variety of oral microorganisms. Differences in the surface characteristics of these materials may affect bacterial adhesion and the accumulation of multispecies biofilms, potentially influencing peri-implant tissue health [11–15].

Unlike periodontitis, which is predominantly associated with a well-characterized group of periodontal pathogens, peri-implant diseases have been shown to involve a more diverse and complex microbial community [16]. Several microorganisms have been implicated in the initiation and progression of peri-implant infections, including classical periodontal pathogens such as *Prevotella intermedia*, and *Porphyromonas gingivalis* and *Treponema denticola*, as well as opportunistic species including *Staphylococcus aureus* and *Candida albicans* [17–19]. The presence of these microorganisms may contribute to biofilm formation, peri-implant mucosal inflammation, and subsequent peri-implant tissue destruction [16–19].

Increased surface roughness of dental resin showed an increase in microbial and bacterial adhesion [20]. In addition, it has been shown that the surface roughness of 3D-printed dental resin showed higher values when compared to the conventional materials [21]. Moreover, studies have shown that the surface topography and properties have been affected by modification of printing parameters and conditions by layering directions [22–26]. In a study that evaluated different printing orientations, no significant changes were noted in surface values with 45- and 90-degree printing orientations when compared to 0-degree; it only demonstrated some variations in values [27].

Although bacterial and microbial accumulation of commercially available titanium, dental composite, and PEEK healing abutments have been extensively investigated, limited evidence exists regarding bacterial adhesion to customized healing abutments fabricated from 3D-printed dental resin. Moreover, the potential effects of the printing orientation on microbial accumulation remain largely unexplored. Therefore, the aim of this in vitro study was to evaluate and compare microbial accumulation on different materials of implant healing abutments, including commercially available titanium stock abutments, customized healing abutments made from dental composite resin, and 3D-printed custom healing abutments. Additionally, the effects of three different printing orientations on the accumulation of these microorganisms were investigated. Two null hypotheses were tested: ($H_0$1) there is no significant difference in microbial accumulation among healing abutments of

different materials and fabrication methods, and ($H_0$2) there is no significant difference in microbial accumulation among 3D-printed healing abutments fabricated at different printing orientations.

2. Materials and Methods

2.1. Sample Size and Study Groups

The required sample size was calculated based on data from a previous study [28] to achieve 90% statistical power with a significance level (α) of 0.05, resulting in a minimum of nine specimens per group. A total of 50 healing abutment specimens were included in this study and allocated into five groups ($n = 10$ per group) as follows; Group I: commercially available pure titanium healing abutments (Straumann AG, Basel, Switzerland; RC Healing Abutment, conical shape, D 5 mm × H 4 mm; (REF 024.4224S)), which served as the control group; Group II: customized healing abutments made directly from dental resin composite (Filtek Supreme Ultra, 3M ESPE, St. Paul, MN, USA) (CHA-Composite); Group III: 3D-printed customized healing abutments fabricated from photopolymerized methaacrylate dental resin (Asiga, Erfurt, Germany) using a 0° printing orientation (CHA-3DP-0); Group IV: 3D-printed customized healing abutments fabricated from photopolymerized methaacrylate dental resin (Asiga, Erfurt, Germany) using a 45° printing orientation (CHA-3DP-45); and Group V: 3D-printed customized healing abutments fabricated from photopolymerized methaacrylate dental resin (Asiga, Erfurt, Germany) using a 90° printing orientation (CHA-3DP-90). Figure 1 presents a summary of materials used and the study flowchart.

2.2. Specimen Preparation of Customized Healing Abutments

A duplicate of the commercially available titanium stock healing abutment was used to standardize the shape, dimensions, and morphology of the customized healing abutments.

For the CHA-Composite group, a silicone putty mold of the titanium stock healing abutment was fabricated using clear vinyl polysiloxane material (Exaclear, GC, Tokyo, Japan). The material was left to set for 7 min according to the manufacturer's instructions. Then, a flowable composite (Filtek Supreme Ultra, 3M ESPE, St. Paul, MN, USA) was gradually used to fill the silicone matrix. A light-curing unit (Valo Cordless, Ultradent, South Jordan, UT, USA) at a power of 800 mW and an irradiance of 1000 mW/cm^2 was used to polymerize the resin for 20 s per side according to the manufacturer's instructions. All specimens were visually examined, and any with a defect or an air bubble were excluded from the study.

For the 3D-printed CHA, the titanium stock healing abutment was scanned using an intraoral scanner (Trios 3, 3shape, Copenhagen, Denmark). The scan was exported as an STL file. The STL file was transferred to a dental 3D printer (ASIGA MAX™, Alexandria, Australia). The Asiga printer is a DLP projector that flashes a full-layer image at once using an industrial-grade UV LED with a wavelength of 385nm. Before printing, 7 support structures were added to the screw side of each specimen (Figure 1). For each group, a DentaTOOTH resin (Photopolymerized Methacrylate; LOT: 18604, Item no. 03625, Asiga Alexandria, Australia) was placed in a shaker (LC-3DMixer, NextDent B.V., Soesterberg, The Netherlands) for 20 min, then used to print the specimens in three different printing orientations (0-, 45-, 90-degree) in a single printing session using identical printing parameters. The layer thickness was standardized at 50 µm in all groups. After printing, the excess material was removed using sharp blades. The specimens were then cleaned with Isopropyl Alcohol 99.9% (Saudi Pharmaceutical Industries, Riyadh, Saudi Arabia) for 10 min. Following cleaning, all specimens underwent the same post-curing treatment involving placing them in Asiga Flash (Asiga, Erfurt, Germany) for 30 min. The Asiga curing unit was a UV

radiation lamp (Type: DR-301C). A summary of all printing parameters and post-printing conditions is presented in Figure 1.

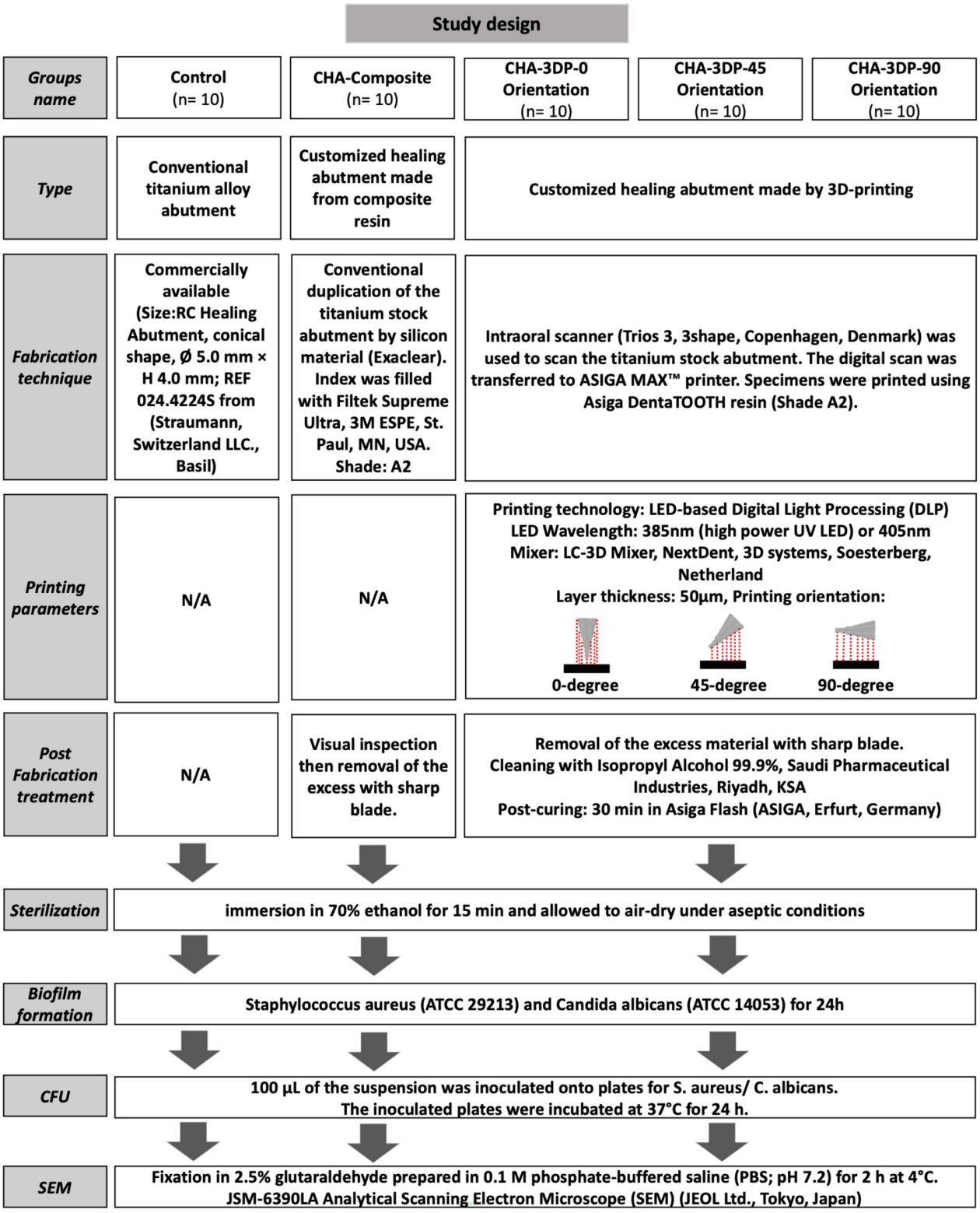

Figure 1. Study flowchart (N/A: not applicable).

2.3. Biofilm Formation

Following fabrication and inspection, the biological specimens were randomly allocated to five experimental groups (n = 10 per group), with specimen identification and group

allocation performed by an investigator who was not involved in the microbiological analysis to minimize allocation bias. Prior to microbial inoculation, all specimens were sterilized by immersion in 70% ethanol for 15 min. Following sterilization, the specimens were thoroughly rinsed three times with sterile phosphate-buffered saline (PBS) to remove residual ethanol and then allowed to air-dry completely under aseptic conditions in a sterile laminar flow hood for 24 h [29]. Standard strains of *Staphylococcus aureus* (ATCC 29213) and *Candida albicans* (ATCC 14053), obtained from the Microbiology Department, College of Medicine at Imam Abdulrahman Bin Faisal University, were cultured according to ATCC-recommended culture protocols. Microbial suspensions were prepared in sterile phosphate-buffered saline (PBS) and adjusted to a turbidity equivalent to the 0.5 McFarland standard according to CLSI guidelines (CLSI M07; CLSI M27). To simulate polymicrobial conditions, *S. aureus* and *C. albicans* were combined to prepare a mixed inoculum. The viable inoculum concentration was experimentally confirmed by culture and CFU enumeration, with a starting concentration of approximately 1.5×10^8 CFU/mL. For biofilm formation, each sterilized specimen was individually placed in a 1.5 mL sterile tube containing Brain Heart Infusion (BHI) broth supplemented with 100 µL of the standardized microbial suspension. The specimens were fully immersed in the BHI broth and incubated statically at 37 °C for 24 h to enable optimal nutrient availability for bacterial growth and robust biofilm development prior to CFU analysis. Biofilm formation was performed using a static incubation model adapted from previously described biomaterial adhesion protocols [30,31]. Following incubation, each specimen was gently rinsed three times with sterile PBS to remove non-adherent microorganisms and transferred to a new sterile microcentrifuge tube containing 1 mL of sterile PBS and subjected to ultrasonication for 5 min. The tubes were then vortexed for 1 min to detach the adherent biofilm from the specimen surface as previously described [30,32]. For quantitative microbial analysis, 100 µL of the resulting suspension was serially diluted and inoculated onto blood agar plates for *S. aureus* and Sabouraud dextrose agar plates for *C. albicans*. The inoculated plates were incubated at 37 °C for 24 h, and microbial growth was subsequently assessed by quantifying the number of colony-forming units (CFUs) as described by Madigan MT et al. [33]. The CFUs were determined by counting the grown colonies in consideration of the dilution factor, following the equation:

$$\text{CFU/mL} = (\text{Number of colonies counted} \times \text{Dilution factor})/\text{Volume plated (mL)}$$

2.4. Scanning Electron Microscopy (SEM)

Following biofilm formation, representative healing abutment specimens were prepared for SEM using JSM-6390LA Analytical SEM (JEOL Ltd., Tokyo, Japan) at the designated magnifications after gold sputter coating using Cressington 108 Auto Sputter Coater (Cressington Scientific Instruments Ltd., Watford, Hertfordshire, UK) to evaluate microbial accumulation and surface biofilm morphology. The specimens were fixed in 2.5% glutaraldehyde prepared in 0.1 M phosphate-buffered saline (PBS; pH 7.2) for 2 h at 4 °C. Following primary fixation, the specimens were rinsed three times with PBS and post-fixed in 1% osmium tetroxide for 1 h. The specimens were subsequently dehydrated through a graded ethanol series (30%, 50%, 70%, 80%, 90%, 95%, and 100%), followed by complete drying. The dehydrated specimens were then sputter-coated with a thin gold layer (approximately 5–10 nm) to enhance electrical conductivity prior to SEM examination according to established biological electron microscopy protocols [34,35]. Similar preparation methods have been widely employed for evaluating microbial biofilms on dental implant biomaterials [36,37]. Two samples per group were subjected to SEM analysis and the spots were selected randomly. SEM images were acquired at different magnifications to qualitatively demonstrate microbial accumulation on the specimen surfaces.

2.5. Statistical Analysis

The normality of the data distribution was evaluated using the Shapiro–Wilk test, and the homogeneity of variances was assessed using Levene's test. Both assumptions were evaluated using the Log10-transformed CFU data prior to performing the parametric analyses. Differences in mean Log_{10} CFU counts per mL among the five experimental groups (Control, Resin Composite, Printed-0° Orientation, Printed-45° Orientation, and Printed-90° Orientation) were analyzed separately for *C. albicans* and *S. aureus* using one-way analysis of variance (ANOVA), followed by Tukey's Honestly Significant Difference (HSD) post hoc test for pairwise comparisons. The two microorganisms were analyzed as independent experimental datasets, and no cross-species interaction was evaluated. Statistical significance was defined as a two-sided p-value < 0.05. All statistical analyses were conducted using SigmaPlot version 16 (Systat Software Inc., San Jose, CA, USA).

3. Results

C. albicans CFUs results are shown in Table 1 and Figure 2. Results of the One-way ANOVA showed that the groups differed significantly ($F = 29.39$, $p < 0.001$). Post hoc Tukey testing showed that the Printed-0° group had significantly lower CFU counts compared to all other groups ($p < 0.001$), while Printed-90° had significantly higher counts than Control, Resin Composite, and Printed-0° ($p < 0.05$).

Table 1. Colony-forming units (Log_{10} CFU/mL) of *Candida albicans* across experimental groups.

Group	Mean (Log_{10})	SD	95% CI
Control	2.976	0.259	[2.791–3.161]
CHA-Composite	2.912	0.357	[2.656–3.167]
CHA-3DP-0 Orientation	1.994	0.460	[1.665–2.323]
CHA-3DP-45 Orientation	3.208	0.317	[2.981–3.434]
CHA-3DP-90 Orientation	3.522	0.221	[3.365–3.680]

SD: Standard deviation; CI: Confidence Interval; CHA: Customized Healing Abutment.

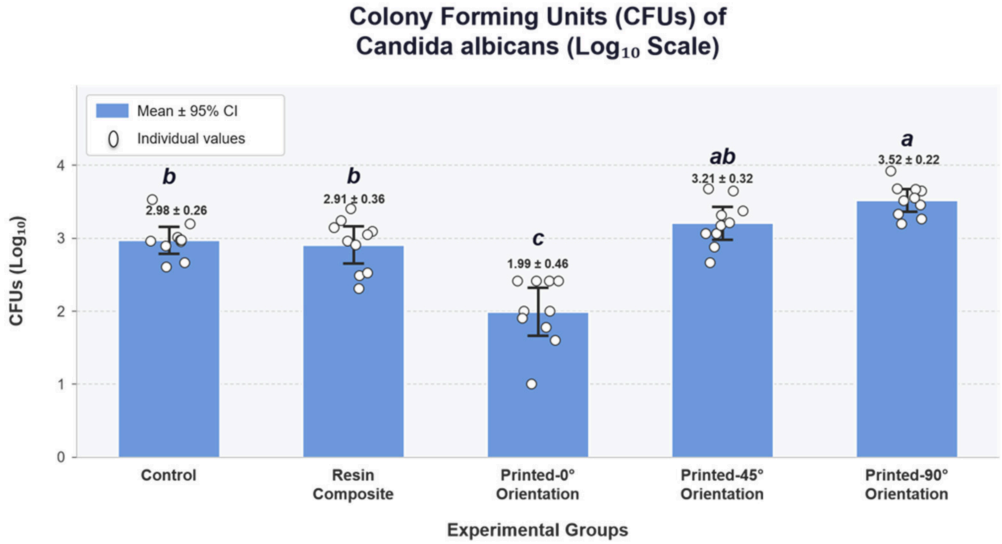

Figure 2. Colony-forming units (Log_{10} CFU/mL) of *Candida albicans* across experimental groups. Mean colony-forming units (CFUs) of *Candida albicans* expressed as Log_{10} values across the five experimental groups (Control, Resin CHA Composite, CHA 3D-Printed-0° Orientation, CHA 3D-Printed-45° Orientation, and CHA 3D-Printed-90° Orientation). Error bars represent 95% confidence intervals. Individual data points are shown as open circles. Different letters above bars indicate statistically significant differences between groups using Tukey's test ($p < 0.05$).

The results of *Staphylococcus aureus* CFUs are shown in Table 2 and Figure 3. Results of the One-way ANOVA showed that the groups differed significantly ($F = 29.54$, $p < 0.001$). Post hoc Tukey testing showed that the Printed-0° group had significantly lower CFU counts compared to all other groups ($p < 0.001$), and the Printed-45° and Printed-90° groups showed significantly higher counts than Control ($p < 0.001$ and $p < 0.001$, respectively).

Table 2. Colony-forming units (Log_{10} CFU/mL) of *Staphylococcus aureus* across experimental groups.

Group	Mean (Log_{10})	SD	95% CI
Control	2.665	0.137	[2.566–2.763]
CHA-Composite	2.901	0.426	[2.596–3.206]
CHA-3DP-0 Orientation	2.003	0.311	[1.781–2.226]
CHA-3DP-45 Orientation	3.209	0.342	[2.964–3.454]
CHA-3DP-90 Orientation	3.447	0.331	[3.210–3.683]

SD: Standard deviation; CI: Confidence interval; CHA: Customized healing abutment.

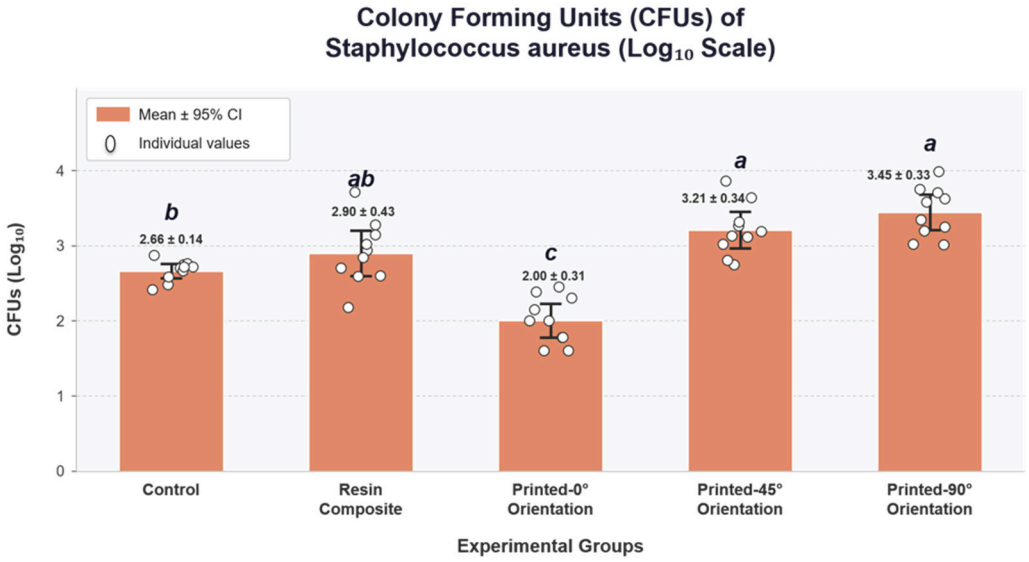

Figure 3. Colony-forming units (Log_{10} CFU/mL) of *Staphylococcus aureus* across experimental groups. Mean colony-forming units (CFUs) of *Staphylococcus aureus* expressed as Log_{10} values across the five experimental groups (Control, Resin CHA Composite, CHA 3D-Printed-0° Orientation, CHA 3D-Printed-45° Orientation, and CHA 3D-Printed-90° Orientation). Error bars represent 95% confidence intervals. Individual data points are shown as open circles. Different letters above bars indicate statistically significant differences between groups using Tukey's test ($p < 0.05$).

SEM examination revealed distinct differences in biofilm formation and surface morphology across the five experimental groups (Figure 4).

The Control group displayed a relatively smooth surface with sparse, isolated clusters of spherical cells, reflecting the moderate CFU counts observed. The resin composite exhibited a surface with numerous adherent microorganisms, including spherical microbial cells, indicating apparent microbial accumulation. The Printed-0° Orientation group showed visible microbial accumulation across the surface, yet it showed notably fewer visible microorganisms Figure 4. Scanning electron microscopy (SEM) images of biofilm formation on the surfaces of the five experimental groups: Control, Resin CHA Composite, CHA 3D-Printed-0° Orientation, CHA 3D-Printed-45° Orientation, and CHA 3D-Printed-90° Orientation. Images were captured at magnifications ranging from ×2500 to ×3000. Scale bars represent 5–10 µm.

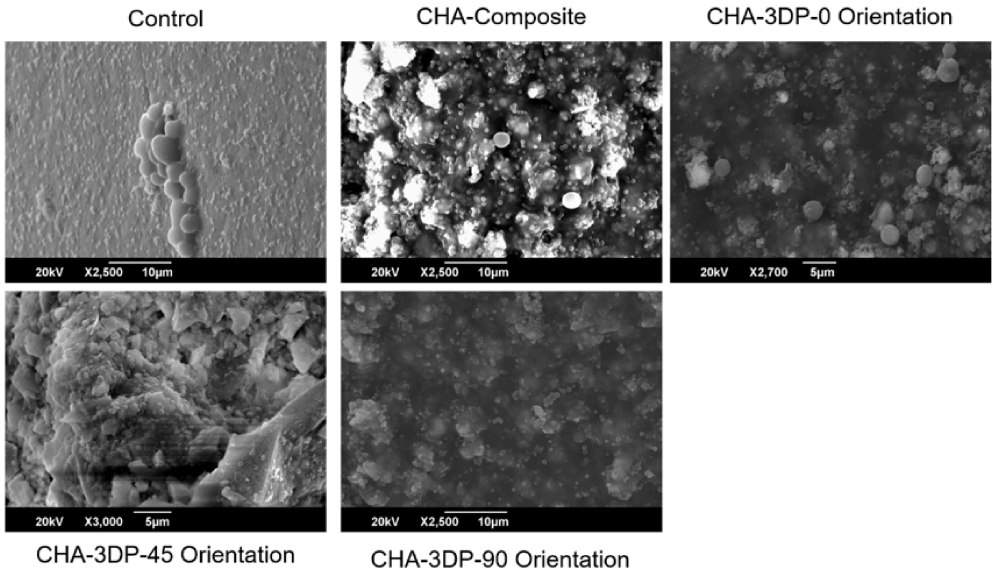

Figure 4. Scanning electron microscopy (SEM) images of biofilm formation on the surfaces of the five experimental groups: Control, Resin CHA Composite, CHA 3D-Printed-0° Orientation, CHA 3D-Printed-45° Orientation, and CHA 3D-Printed-90° Orientation. Images were captured at magnifications ranging from ×2500 to ×3000. Scale bars represent 5–10 µm.

Relative to the Resin Composite group. The Printed-45° Orientation group showed the most complex surface topography change among the 3D-printed groups, featuring irregular, laminated surface layers with biofilm formation. The rough, folded surface architecture likely promotes microbial entrapment and retention, which corresponds to the high CFU counts observed for this group (mean Log_{10} = 3.208 for *C. albicans*; 3.209 for *S. aureus*), exceeding those of the Printed-0° group. The Printed-90° Orientation group presented a uniformly distributed pattern of spherical microbial cells across a relatively homogeneous surface, with a widespread microbial presence.

4. Discussion

The findings of the present study demonstrated that microbial accumulation varied among healing abutments fabricated from different materials. Furthermore, the printing orientation of CHAs influenced microbial accumulation, suggesting that both material composition and surface characteristics contribute to the initial establishment of peri-implant biofilms. Therefore, both null hypotheses were rejected.

Although numerous in vitro studies have investigated bacterial adhesion to various implant and healing abutment materials [12,14,15,36,38], only a limited number have specifically evaluated clinically relevant peri-implant pathogens such as *Staphylococcus aureus* and *Candida albicans* [12,17–19,38–41]. Therefore, *S. aureus* and *C. albicans* were selected as clinically relevant opportunistic microorganisms frequently associated with implant-related infections, while acknowledging that single-species models do not fully represent the complexity of the polymicrobial peri-implant biofilm. Moreover, the available literature has primarily focused on comparisons between conventional materials, with little attention given to CHAs. To the best of the authors' knowledge, no published study has specifically investigated the influence of different printing orientations on microbial adhesion to CHAs. While previous studies have evaluated microbial adhesion on CAD-CAM PMMA materials [12,15,36,38] or described the fabrication of customized PMMA healing abutments [2,5,42], the effect of printing orientation on biofilm formation has not been investigated.

Therefore, the present study provides novel in vitro evidence on the biofilm formation of *S. aureus* and *C. albicans* on customized healing abutments fabricated from titanium, resin composite, and 3D-printed resin, with particular emphasis on the influence of build orientation on the microbial accumulation characteristics of 3D-printed customized healing abutments. These findings suggest that both the choice of healing abutment material and the fabrication methods may influence microbial accumulation and could be considered when designing and manufacturing CHAs to minimize the risk of peri-implant biofilm formation.

The findings demonstrated that microbial accumulation differed significantly among the tested materials and fabrication protocols. Notably, 3D Printing-CHA in the 0° orientation exhibited the lowest biofilm accumulation for both microorganisms, whereas the 45° group and, particularly, the 90° group orientations demonstrated significantly greater microbial accumulation.

Microbial adhesion to dental material surfaces is a multifactorial process influenced by surface roughness, surface free energy, wettability, chemical composition, and surface topography [43,44]. In particular, investigations of 3D-printed dental polymers have reported orientation-dependent differences in microbial adhesion, including comparisons among 0°, 45°, and 90° build orientations. Previous investigations have consistently demonstrated that even subtle alterations in surface morphology, in terms of polished surfaces among different materials, can affect the initial adhesion of microorganisms and subsequent biofilm maturation [45–49]. Because the 3D-printed method generates characteristic machining grooves and tool marks [50,51] different printing orientations are expected to produce distinct surface textures despite the use of the same 3D-printable resin material. Consequently, differences in microbial accumulation observed in the present study are likely attributable primarily to variations in surface topography created by the printing direction rather than differences in the bulk material itself.

The remarkably lower microbial accumulation observed in the CHA-3DP-0 group suggests that this printing orientation may produce a smoother and more homogeneous surface with fewer irregularities, thereby reducing favorable sites for microbial retention and initial accumulation. In contrast, the greater biofilm accumulation observed in the CHA-3DP-45 and CHA-3DP-90 groups may be associated with build-orientation-dependent surface features, such as more pronounced layer lines, surface irregularities, and microscopic undercuts. These features may provide additional sites or sheltered niches for microbial attachment and retention [37]. The relationship between surface roughness and microbial adhesion is not strictly linear; microbial adhesion also depends on material chemistry, surface energy, and wettability, meaning that roughness interacts with these factors [52]. Evidence also indicates that surface roughness alone is not the primary determinant of microbial behavior, as several studies report no significant influence of topography on *C. albicans* adhesion, biofilm formation, or morphological expression [53]. However, as surface morphology was assessed qualitatively by SEM, quantitative characterization is needed to confirm whether these surface features contribute to the observed differences in microbial adhesion and biofilm formation.

These observations were supported by SEM analysis. The CHA-3DP-0 specimens demonstrated relatively limited biofilm accumulation compared with the other 3D-printed groups, whereas the CHA-3DP-45 orientation exhibited irregular laminated surface features associated with extensive microbial accumulation. Similarly, the CHA-3DP-90 orientation showed a uniformly distributed biofilm covering the surface. The consistency between the quantitative CFU measurements and the qualitative SEM observations supports the overall findings of the present study. The observed differences in microbial accumulation were associated with the different printing orientations, while the qualitative SEM images suggest that variations in surface topography may be one possible contributing mechanism.

However, quantitative characterization of surface morphology is required to confirm the relationship between surface characteristics and microbial adhesion. Although titanium has long been considered the gold standard for healing abutments because of its favorable biocompatibility and corrosion resistance [54,55] microbial adhesion to titanium surfaces remains inevitable within the oral environment, as explained in several studies [36,43,44,56]. Previous studies have reported variable bacterial adhesion to titanium depending on surface treatment [57], surface roughness, and polishing procedures [36,56,58]. In addition, several studies have demonstrated that clinically used and re-sterilized healing abutments frequently retain residual proteins, organic debris, and biofilm remnants. These residual surface contaminants may modify the titanium surface and create irregularities for subsequent microbial adhesion compared with new healing abutments [59–61]. In the present study, the commercially available new titanium healing abutments demonstrated intermediate levels of microbial accumulation, which were considered significantly lower than those in the CHA-3DP-45 and CHA-3DP-90 groups but higher than those in the CHA-3DP-0 specimens. These findings suggest that optimized 3D-printing orientation may influence early microbial accumulation under static in vitro conditions; however, further studies are required to determine its implications for clinical performance and other biological and mechanical properties. The resin composite healing abutments demonstrated microbial accumulation levels comparable to those observed for titanium groups in both microbial species. Composite materials contain an organic resin matrix that may undergo surface degradation, water sorption, and filler particle exposure during aging, potentially increasing surface roughness and promoting microbial attachment [46,62–64]. The SEM findings in the present study demonstrated areas of matrix degradation associated with dense microbial accumulation, supporting previous reports that surface deterioration of resin-based materials may facilitate biofilm development.

Both *Candida albicans* and *Staphylococcus aureus* exhibited remarkably similar accumulation patterns across the experimental groups. Despite their biological differences, both microorganisms demonstrated significantly reduced microbial accumulation on the CHA-3DP-0 surfaces and increased microbial accumulation on the CHA-3DP-45 and CHA-3DP-90 orientations. This consistent trend suggests that the influence of surface topography generated by printing orientation may represent a dominant factor governing initial microbial attachment irrespective of microbial species. The inclusion of both a fungal and a bacterial pathogen enhances the clinical relevance of the present findings because these microorganisms have been implicated in peri-implant infections, particularly in medically compromised patients and individuals with established peri-implant disease [17–19].

It should be noted that, since the titanium, composite resin, and printed resin groups differed simultaneously in both material composition and manufacturing process, the observed differences among these groups should be interpreted as reflecting specific material–manufacturing process combinations rather than the independent effect of either factor alone.

It is important to note that artificial saliva has been shown to influence the microstructural and mechanical behavior of resin-based CAD/CAM materials through water sorption and hydrolytic degradation of the polymer matrix, potentially affecting surface roughness and microbial colonization. These saliva-mediated effects may modulate the resin-microbe interactions and biofilm formation dynamics and their absence in the present study is considered a major limitation.

Several limitations of the present study should be acknowledged. First, this was an in vitro study performed under controlled laboratory conditions and therefore may not fully replicate the complex oral environment, including salivary pellicle formation, host immune responses, masticatory loading, and dynamic fluid conditions. Second, only two

representative peri-implant microorganisms were evaluated using a single-species model, whereas peri-implant biofilms are composed of diverse polymicrobial communities; therefore, the present findings may not reflect microbial interactions occurring in vivo. Third, the observation period was limited to 24 h, and the resin materials were not subjected to aging, which may influence their surface characteristics and microbial accumulation over longer periods. Fourth, surface roughness, surface free energy, wettability, and quantitative surface topography were not directly measured, and SEM assessment was qualitative. Consequently, the proposed relationship between printing orientation, surface characteristics, and microbial accumulation should be considered a possible explanation rather than a confirmed causal mechanism. Fifth, the potential effects of the specimen cleaning and sterilization procedures, including ethanol exposure, on resin surface characteristics or degree of conversion were not independently evaluated and cannot be excluded. In addition, the sterilization protocol was not independently validated for each material. Sixth, the customized healing abutment dimensions used in this study were based on a replica of a stock titanium alloy healing abutment and may not represent the range of dimensions and geometries of customized healing abutments used clinically. Future studies should incorporate quantitative surface characterization techniques, such as surface profilometry, atomic force microscopy, and contact-angle measurements, together with dynamic and polymicrobial biofilm models, salivary pellicle formation, and material-aging protocols. Such studies would help clarify the relationship between 3D-printing orientation, surface characteristics, and microbial colonization. Clinical investigations are also warranted to determine whether the observed in vitro differences translate into improved peri-implant soft-tissue health and clinical outcomes.

5. Conclusions

The present study demonstrates that both healing abutment material and 3D printing orientation significantly influence early microbial accumulation. Among the tested groups, the CHA-3DP-0 group exhibited the lowest microbial accumulation by *Staphylococcus aureus* and *Candida albicans*. Further in vitro and in vivo studies using quantitative surface characterization and more representative biofilm models are required to confirm the translational relevance of these findings.

Funding: This research received no external funding.

Institutional Review Board Statement: Not applicable.

Informed Consent Statement: Not applicable.

Data Availability Statement: The raw data supporting the conclusions of this article will be made available by the author on request.

Acknowledgments: The author would like to express their sincere appreciation to Yousif AlDulaijan, Department of Substitutive Dental Sciences, College of Dentistry, Imam Abdulrahman Bin Faisal University, for his valuable review of the manuscript. The author also thanks Abdulrahman Balhaddad, Department of Restorative Dental Sciences, College of Dentistry, Imam Abdulrahman Bin Faisal University, for his valuable assistance with statistical analysis. Special thanks are extended to Badr Saker, Laboratory Technician, for his assistance with the microbiological culture procedures and Raju Thangaruju for his assistance in preparing the specimens.

Conflicts of Interest: The author declares no conflicts of interest.

Abbreviations

The following abbreviations are used in this manuscript:

3D	Three-dimensional
CAD-CAM	Computer-Aided Design and Computer-Aided Manufacturing
C. albicans	*Candida albicans*
CFU	Colony-Forming Unit
CHA	Customized Healing Abutment
CHA-Composite	Customized Composite Resin Healing Abutment
CHA-3DP-0	Customized 3D-Printed Healing Abutment (0° Printing Orientation)
CHA-3DP-45	Customized 3D-Printed Healing Abutment (45° Printing Orientation)
CHA-3DP-90	Customized 3D-Printed Healing Abutment (90° Printing Orientation)
PBS	Phosphate-Buffered Saline
PEEK	Polyetheretherketone
PMMA	Poly(methyl methacrylate)
SEM	Scanning Electron Microscopy
S. aureus	*Staphylococcus aureus*

References

1. Jung, R.E.; Zembic, A.; Pjetursson, B.E.; Zwahlen, M.; Thoma, D.S. Systematic Review of the Survival Rate and the Incidence of Biological, Technical, and Aesthetic Complications of Single Crowns on Implants Reported in Longitudinal Studies with a Mean Follow-up of 5 Years. *Clin. Oral Implants Res.* **2012**, *23*, 2–21. [CrossRef] [PubMed]
2. Pow, E.H.; McMillan, A.S. A Modified Implant Healing Abutment to Optimize Soft Tissue Contours: A Case Report. *Implant Dent.* **2004**, *13*, 297–300. [CrossRef] [PubMed]
3. Elian, N.; Tabourian, G.; Jalbout, Z.N.; Classi, A.; Cho, S.; Froum, S.; Tarnow, D.P. Accurate Transfer of Peri-implant Soft Tissue Emergence Profile from the Provisional Crown to the Final Prosthesis Using an Emergence Profile Cast. *J. Esthet. Restor. Dent.* **2007**, *19*, 306–314. [CrossRef] [PubMed]
4. Janakievski, J. Case Report: Maintenance of Gingival Form Following Immediate Implant Placement—The Custom-Healing Abutment. *Adv. Esthet. Interdiscip. Dent.* **2007**, *3*, 24–28.
5. Proussaefs, P. Use of CAD/CAM Healing Abutment Immediately after Dental Implant Placement for the Non-Esthetic Zone: A Guided Soft Tissue Healing Technique. *J. Oral Implantol.* **2016**, *42*, 189–193. [CrossRef] [PubMed]
6. Berglundh, T.; Abrahamsson, I.; Welander, M.; Lang, N.P.; Lindhe, J. Morphogenesis of the Peri-implant Mucosa: An Experimental Study in Dogs. *Clin. Oral Implants Res.* **2007**, *18*, 1–8. [CrossRef] [PubMed]
7. Berglundh, T.; Lindhe, J.; Ericsson, I.; Marinello, C.P.; Liljenberg, B.; Thornsen, P. The Soft Tissue Barrier at Implants and Teeth. *Clin. Oral Implants Res.* **1991**, *2*, 81–90. [CrossRef] [PubMed]
8. Prati, C.; Zamparini, F.; Canullo, L.; Pirani, C.; Botticelli, D.; Gandolfi, M.G. Factors Affecting Soft and Hard Tissues around Two-Pies Transmucosal Implants: A 3-Year Prospective Cohort Study. *Int. J. Oral Maxillofac. Implants* **2020**, *35*, 1022–1036. [CrossRef] [PubMed]
9. Chokaree, P.; Poovarodom, P.; Chaijareenont, P.; Yavirach, A.; Rungsiyakull, P. Biomaterials and Clinical Applications of Customized Healing Abutment—A Narrative Review. *J. Funct. Biomater.* **2022**, *13*, 291. [CrossRef] [PubMed]
10. Osman, R.B.; Swain, M.V. A Critical Review of Dental Implant Materials with an Emphasis on Titanium versus Zirconia. *Materials* **2015**, *8*, 932–958. [CrossRef] [PubMed]
11. Dorkhan, M.; Hall, J.; Uvdal, P.; Sandell, A.; Svensäter, G.; Davies, J.R. Crystalline Anatase-Rich Titanium Can Reduce Adherence of Oral Streptococci. *Biofouling* **2014**, *30*, 751–759. [CrossRef] [PubMed]
12. Hung, C.C.U.; Costa, R.C.; Pereira, G.; Abdo, V.L.; do Santos Noronha, M.; Retamal-Valdes, B.; Bertolini, M.; Feres, M.; Shibli, J.A.; Barão, V.A.; et al. Oral Microbial Colonization on Titanium and Polyetheretherketone Dental Implant Healing Abutments: An in Vitro and in Vivo Study. *J. Prosthet. Dent.* **2025**, *133*, 1545–1552. [CrossRef] [PubMed]
13. Chrcanovic, B.R.; Kisch, J.; Albrektsson, T.; Wennerberg, A. Factors Influencing Early Dental Implant Failures. *J. Dent. Res.* **2016**, *95*, 995–1002. [CrossRef] [PubMed]
14. D'Ercole, S.; Piattelli, A.; Marzo, G.; Scarano, A.; Tripodi, D. Influence of Bacterial Colonization of the Healing Screws on Peri-Implant Tissue. *J. Dent. Sci.* **2013**, *8*, 109–114. [CrossRef]
15. Jain, S.S.; Schramm, S.T.; Siddiqui, D.A.; Huo, W.; Palmer, K.L.; Wilson, T.G., Jr.; Rodrigues, D.C. Effects of Multiple Implantations of Titanium Healing Abutments: Surface Characteristics and Microbial Colonization. *Dent. Mater.* **2020**, *36*, e279–e291. [CrossRef] [PubMed]

16. Kumar, P.S.; Mason, M.R.; Brooker, M.R.; O'Brien, K. Pyrosequencing Reveals Unique Microbial Signatures Associated with Healthy and Failing Dental Implants. *J. Clin. Periodontol.* **2012**, *39*, 425–433. [CrossRef] [PubMed]
17. Leonhardt, Å.; Renvert, S.; Dahlén, G. Microbial Findings at Failing Implants. *Clin. Oral Implants Res.* **1999**, *10*, 339–345. [CrossRef] [PubMed]
18. Fragkioudakis, I.; Konstantopoulos, G.; Kottaridi, C.; Doufexi, A.-E.; Sakellari, D. Quantitative Assessment of *Candida albicans*, *Staphylococcus aureus* and *Staphylococcus epidermidis* in Peri-Implant Health and Disease: Correlation with Clinical Parameters. *J. Med. Microbiol.* **2024**, *73*, 001933. [CrossRef] [PubMed]
19. Albertini, M.; López-Cerero, L.; O'Sullivan, M.G.; Chereguini, C.F.; Ballesta, S.; Ríos, V.; Herrero-Climent, M.; Bullón, P. Assessment of Periodontal and Opportunistic Flora in Patients with Peri-implantitis. *Clin. Oral Implants Res.* **2015**, *26*, 937–941. [CrossRef] [PubMed]
20. Gad, M.M.; Fouda, S.M. Current Perspectives and the Future of *Candida albicans*-Associated Denture Stomatitis Treatment. *Dent. Med. Probl.* **2020**, *57*, 95–102. [CrossRef] [PubMed]
21. Al-Dulaijan, Y.A.; Alsulaimi, L.; Alotaibi, R.; Alboainain, A.; Alalawi, H.; Alshehri, S.; Khan, S.Q.; Alsaloum, M.; AlRumaih, H.S.; Alhumaidan, A.A.; et al. Comparative Evaluation of Surface Roughness and Hardness of 3D Printed Resins. *Materials* **2022**, *15*, 6822. [CrossRef] [PubMed]
22. Keßler, A.; Hickel, R.; Ilie, N. In Vitro Investigation of the Influence of Printing Direction on the Flexural Strength, Flexural Modulus and Fractographic Analysis of 3D-Printed Temporary Materials. *Dent. Mater. J.* **2021**, *40*, 641–649. [CrossRef] [PubMed]
23. Letcher, T.; Waytashek, M. Material Property Testing of 3D-Printed Specimen in PLA on an Entry-Level 3D Printer. In *Proceedings of the ASME International Mechanical Engineering Congress and Exposition, Montreal, QC, Canada, 14–20 November 2014*; American Society of Mechanical Engineers: New York City, NY, USA, 2014; Volume 46438, p. V02AT02A014.
24. Tymrak, B.M.; Kreiger, M.; Pearce, J.M. Mechanical Properties of Components Fabricated with Open-Source 3-D Printers under Realistic Environmental Conditions. *Mater. Des.* **2014**, *58*, 242–246. [CrossRef]
25. Unkovskiy, A.; Bui, P.H.-B.; Schille, C.; Geis-Gerstorfer, J.; Huettig, F.; Spintzyk, S. Objects Build Orientation, Positioning, and Curing Influence Dimensional Accuracy and Flexural Properties of Stereolithographically Printed Resin. *Dent. Mater.* **2018**, *34*, e324–e333. [CrossRef] [PubMed]
26. Tian, Y.; Chen, C.; Xu, X.; Wang, J.; Hou, X.; Li, K.; Lu, X.; Shi, H.; Lee, E.-S.; Jiang, H.B. A Review of 3D Printing in Dentistry: Technologies, Affecting Factors, and Applications. *Scanning* **2021**, *2021*, 9950131. [CrossRef] [PubMed]
27. Shim, J.S.; Kim, J.-E.; Jeong, S.H.; Choi, Y.J.; Ryu, J.J. Printing Accuracy, Mechanical Properties, Surface Characteristics, and Microbial Adhesion of 3D-Printed Resins with Various Printing Orientations. *J. Prosthet. Dent.* **2020**, *124*, 468–475. [CrossRef] [PubMed]
28. Naghsh, N.; Hosseini, A.; Mogharehabed, A.; Yaghini, J.; Pezeshki, Z.; Khaleghi, N. A Comparison of Four Decontamination Procedures in Reusing Healing Abutments: An in Vitro Study. *Saudi Dent. J.* **2024**, *36*, 1141–1145. [CrossRef] [PubMed]
29. Del Hougne, M.; Mitzscherling, A.; Ewald, A.; Schilling, T.; Stahlhut, P.; Gbureck, U.; Schmitter, M. In Vitro Biofilm Formation on 3D-Printed, Milled, and Conventionally Manufactured Denture Base Resins. *Bioengineering* **2026**, *13*, 424. [CrossRef] [PubMed]
30. An, Y.H.; Friedman, R.J. Concise Review of Mechanisms of Bacterial Adhesion to Biomaterial Surfaces. *J. Biomed. Mater. Res.* **1998**, *43*, 338–348. [CrossRef]
31. Donlan, R.M.; Costerton, J.W. Biofilms: Survival Mechanisms of Clinically Relevant Microorganisms. *Clin. Microbiol. Rev.* **2002**, *15*, 167–193. [CrossRef] [PubMed]
32. Azeredo, J.; Azevedo, N.F.; Briandet, R.; Cerca, N.; Coenye, T.; Costa, A.R.; Desvaux, M.; Di Bonaventura, G.; Hébraud, M.; Jaglic, Z.; et al. Critical Review on Biofilm Methods. *Crit. Rev. Microbiol.* **2017**, *43*, 313–351. [CrossRef] [PubMed]
33. Madigan, M.T.; Martinko, J.M.; Parker, J. *Brock Biology of Microorganisms*; Prentice Hall: Upper Saddle River, NJ, USA, 1997; Volume 11.
34. Bozzola, J.J.; Russell, L.D. *Electron Microscopy: Principles and Techniques for Biologists*; Jones & Bartlett Learning: Burlington, MA, USA, 1999.
35. Hayat, M.A. Loss of Antigenicity on Stored Paraffin Sections. *Microsc. Today* **2000**, *8*, 30–32.
36. Teughels, W.; Van Assche, N.; Sliepen, I.; Quirynen, M. Effect of Material Characteristics and/or Surface Topography on Biofilm Development. *Clin. Oral Implants Res.* **2006**, *17*, 68–81. [CrossRef] [PubMed]
37. Quirynen, M.; Bollen, C.M.L. The Influence of Surface Roughness and Surface-free Energy on Supra- and Subgingival Plaque Formation in Man: A Review of the Literature. *J. Clin. Periodontol.* **1995**, *22*, 1–14. [CrossRef] [PubMed]
38. Taşın, S.; Güvenir, M.; Ismatullaev, A. Effects of Surface Characteristics of Conventionally Manufactured, CAD/CAM Milled, and 3D-Printed Interim Materials on Adherence of Streptococcus Mutans and *Candida albicans*. *Cumhur. Dent. J.* **2023**, *26*, 227–234.
39. Bravo, E.; Arce, M.; Ribeiro-Vidal, H.; Herrera, D.; Sanz, M. The Impact of *Candida albicans* in the Development, Kinetics, Structure, and Cell Viability of Biofilms on Implant Surfaces—An in Vitro Study with a Validated Multispecies Biofilm Model. *Int. J. Mol. Sci.* **2024**, *25*, 3277. [CrossRef] [PubMed]

40. Eguia, A.; Arakistain, A.; De-la-Pinta, I.; López-Vicente, J.; Sevillano, E.; Quindós, G.; Eraso, E. *Candida albicans* Biofilms on Different Materials for Manufacturing Implant Abutments and Prostheses. *Med. Oral Patol. Oral Cir. Bucal* **2019**, *25*, e13–e20. [CrossRef] [PubMed]
41. Gökmenoglu, C.; Kara, N.B.; Beldüz, M.; Kamburoğlu, A.; Tosun, İ.; Sadik, E.; Kara, C. Evaluation of *Candida albicans* Biofilm Formation on Various Parts of Implant Material Surfaces. *Niger. J. Clin. Pract.* **2018**, *21*, 33–37. [CrossRef] [PubMed]
42. Raheem, I.M.A.; Hammad, I.A.; Kader, S.H.A.; Fahmy, R.A. Fabrication of a CAD-CAM Custom Healing Abutment Guided by a Conventional Dental Radiograph for Delayed Loaded Dental Implants: A Dental Technique. *J. Prosthet. Dent.* **2022**, *127*, 49–54. [CrossRef] [PubMed]
43. Han, A.; Tsoi, J.K.; Rodrigues, F.P.; Leprince, J.G.; Palin, W.M. Bacterial Adhesion Mechanisms on Dental Implant Surfaces and the Influencing Factors. *Int. J. Adhes. Adhes.* **2016**, *69*, 58–71. [CrossRef]
44. Subramani, K.; E Jung, R.; Molenberg, A.; Hämmerle, C.H. Biofilm on Dental Implants: A Review of the Literature. *Int. J. Oral Maxillofac. Implants* **2009**, *24*, 616–626.
45. Kearns, V.R.; Williams, R.L.; Mirvakily, F.; Doherty, P.J.; Martin, N. Guided Gingival Fibroblast Attachment to Titanium Surfaces: An in Vitro Study. *J. Clin. Periodontol.* **2013**, *40*, 99–108. [CrossRef] [PubMed]
46. Bollenl, C.M.; Lambrechts, P.; Quirynen, M. Comparison of Surface Roughness of Oral Hard Materials to the Threshold Surface Roughness for Bacterial Plaque Retention: A Review of the Literature. *Dent. Mater.* **1997**, *13*, 258–269. [CrossRef] [PubMed]
47. Linkevicius, T.; Valantiejiene, V.; Alkimavicius, J.; Gineviciute, E.; Andrijauskas, R.; Linkeviciene, L. The Effect of a Polishing Protocol on the Surface Roughness of Zirconium Oxide. *Int. J. Prosthodont.* **2020**, *33*, 217–223. [CrossRef] [PubMed]
48. Al-Radha, A.S.D.; Dymock, D.; Younes, C.; O'Sullivan, D. Surface Properties of Titanium and Zirconia Dental Implant Materials and Their Effect on Bacterial Adhesion. *J. Dent.* **2012**, *40*, 146–153. [CrossRef] [PubMed]
49. Batak, B.; Çakmak, G.; Johnston, W.M.; Yilmaz, B. Surface Roughness of High-Performance Polymers Used for Fixed Implant-Supported Prostheses. *J. Prosthet. Dent.* **2021**, *126*, 254.e1–254.e6. [CrossRef] [PubMed]
50. Alfouzan, A.; Alnouwaisar, A.; Alazzam, N.; AL-Otaibi, H.; Labban, N.; Alswaidan, M.; AL-Taweel, S.; Alshehri, H. Surface Roughness Analysis of Prepolymerized CAD/CAM Dental Acrylic Resins Following Combined Surface Treatments. *Mater. Sci.-Pol.* **2021**, *39*, 209–218. [CrossRef]
51. Herráez-Galindo, C.; Rizo-Gorrita, M.; Luna-Oliva, I.; Serrera-Figallo, M.-Á.; Castillo-Oyagüe, R.; Torres-Lagares, D. In Vitro Comparative Study of Fibroblastic Behaviour on Polymethacrylate (PMMA) and Lithium Disilicate Polymer Surfaces. *Polymers* **2019**, *11*, 744. [CrossRef] [PubMed]
52. da Silva, M.D.D.; Nunes, T.S.B.S.; do Viotto, H.E.C.; Coelho, S.R.G.; de Souza, R.F.; Pero, A.C. Microbial Adhesion and Biofilm Formation by *Candida albicans* on 3D-Printed Denture Base Resins. *PLoS ONE* **2023**, *18*, e0292430. [CrossRef] [PubMed]
53. Gendreau, L.; Loewy, Z.G. Epidemiology and Etiology of Denture Stomatitis. *J. Prosthodont.* **2011**, *20*, 251–260. [CrossRef] [PubMed]
54. Albrektsson, T.; Brånemark, P.-I.; Hansson, H.-A.; Lindström, J. Osseointegrated Titanium Implants: Requirements for Ensuring a Long-Lasting, Direct Bone-to-Implant Anchorage in Man. *Acta Orthop. Scand.* **1981**, *52*, 155–170. [CrossRef] [PubMed]
55. Koutouzis, T.; Richardson, J.; Lundgren, T. Comparative Soft and Hard Tissue Responses to Titanium and Polymer Healing Abutments. *J. Oral Implantol.* **2011**, *37*, 174–182. [CrossRef] [PubMed]
56. Yeo, I.-S.; Kim, H.-Y.; Lim, K.S.; Han, J.-S. Implant Surface Factors and Bacterial Adhesion: A Review of the Literature. *Int. J. Artif. Organs* **2012**, *35*, 762–772. [CrossRef] [PubMed]
57. Chen, C.-J.; Ding, S.-J.; Chen, C.-C. Effects of Surface Conditions of Titanium Dental Implants on Bacterial Adhesion. *Photomed. Laser Surg.* **2016**, *34*, 379–388. [CrossRef] [PubMed]
58. Costa, R.C.; Nagay, B.E.; Bertolini, M.; Costa-Oliveira, B.E.; Sampaio, A.A.; Retamal-Valdes, B.; Shibli, J.A.; Feres, M.; Barao, V.A.; Souza, J.G.S. Fitting Pieces into the Puzzle: The Impact of Titanium-Based Dental Implant Surface Modifications on Bacterial Accumulation and Polymicrobial Infections. *Adv. Colloid Interface Sci.* **2021**, *298*, 102551. [CrossRef] [PubMed]
59. Burioni, R.; Silvestrini, L.; D'Orto, B.; Tetè, G.; Nagni, M.; Polizzi, E.; Gherlone, E.F. Could Dental Material Reuse Play a Significant Role in Preservation of Raw Materials, Water, Energy, and Costs? Microbiological Analysis of New versus Reused Healing Abutments: An In Vitro Study. *Bioengineering* **2024**, *11*, 387. [CrossRef] [PubMed]
60. Wadhwani, C.; Schonnenbaum, T.R.; Audia, F.; Chung, K. In-Vitro Study of the Contamination Remaining on Used Healing Abutments after Cleaning and Sterilizing in Dental Practice. *Clin. Implant Dent. Relat. Res.* **2016**, *18*, 1069–1074. [CrossRef] [PubMed]
61. Barreiros, P.; Braga, J.; Faria-Almeida, R.; Coelho, C.; Teughels, W.; Souza, J.C.M. Remnant Oral Biofilm and Microorganisms after Autoclaving Sterilization of Retrieved Healing Abutments. *J. Periodontal Res.* **2021**, *56*, 415–422. [CrossRef] [PubMed]
62. Münchow, E.A.; Ferreira, A.C.A.; Machado, R.M.; Ramos, T.S.; Rodrigues-Junior, S.A.; Zanchi, C.H. Effect of Acidic Solutions on the Surface Degradation of a Micro-Hybrid Composite Resin. *Braz. Dent. J.* **2014**, *25*, 321–326. [CrossRef] [PubMed]

63. Ferracane, J.L. Resin Composite—State of the Art. *Dent. Mater.* **2011**, *27*, 29–38. [CrossRef] [PubMed]
64. Ferracane, J.L. Hygroscopic and Hydrolytic Effects in Dental Polymer Networks. *Dent. Mater.* **2006**, *22*, 211–222. [CrossRef] [PubMed]

Disclaimer/Publisher's Note: The statements, opinions and data contained in all publications are solely those of the individual author(s) and contributor(s) and not of MDPI and/or the editor(s). MDPI and/or the editor(s) disclaim responsibility for any injury to people or property resulting from any ideas, methods, instructions or products referred to in the content.